

CAR-TR-696
CS-TR-3177

F49620-92-J0130
DACA 76-92-C-0024
November 1993

CFAR Detection of Targets in Fully Polarimetric SAR Images

Ying Wang*
Rama Chellappa[†]
Qinfen Zheng[‡]

Computer Vision Laboratory
Center for Automation Research
University of Maryland
College Park, MD 20742-3275

Abstract

Traditional constant false alarm rate (CFAR) detection algorithms produce a lot of false targets when applied to single-look, high-resolution, fully polarimetric synthetic aperture radar (SAR) images, due to the presence of speckle. We propose a two stage CFAR detector followed by conditional dilation for detecting point and extended targets in polarimetric SAR images. In the first stage, possible targets are detected and false targets due to the speckle are removed by using global statistical parameters. In the second stage, the local statistical parameters are used to detect targets in regions adjacent to targets detected in the first stage. Conditional dilation is then performed to recover target pixels lost in second stage CFAR detection.

The performance of a CFAR detector will be degraded if an incorrect statistical model is adopted and the data are correlated. A goodness-of-fit test is performed to decide the appropriate distribution and the effects of decorrelation of the data are considered.

Good experimental results are obtained when our method is applied to single-look, high-resolution, fully polarimetric SAR images acquired from MIT Lincoln Laboratory.

*The first author gratefully acknowledges the support of the K. C. Wong Education Foundation, Hong Kong. Permanent address: Institute of Automation, Chinese Academy of Sciences, Beijing 100080, China.

[†]The second author is supported by the Air Force Office of Scientific Research under Contract F49620-92-J0130.

[‡]The third author is supported by the Advanced Research Projects Agency (ARPA Order 8979) and the U.S. Army Topographic Engineering Center under Contract DACA-76-92-C-0024.

1 INTRODUCTION

In automatic target recognition (ATR) applications, features that distinguish targets from the background and recognition criteria are the two key issues to be resolved. In single channel SAR images, backscattering amplitude is used for target detection and it is usually assumed that strong backscattering comes from targets. A target will be lost when the backscattering amplitude from the target is not large enough compared with the background at some aspect angles [1]. To overcome this, fully polarimetric SAR images are used. The value at every pixel of a polarimetric SAR image is a four-element complex vector. Usually, a three-element complex vector

$$\begin{aligned} \underline{X} &= \begin{bmatrix} HH \\ HV \\ VV \end{bmatrix} \\ &= \begin{bmatrix} HH_i + jHH_q \\ HV_i + jHV_q \\ VV_i + jVV_q \end{bmatrix} \end{aligned} \quad (1)$$

is used according to the reciprocity principle [2]. In (1), $j = \sqrt{-1}$, and the real and imaginary parts are the in-phase and quadrature components. The ensemble average of every element is zero and the polarimetric covariance matrix is

$$\Sigma = \begin{bmatrix} \langle HH, HH \rangle & \langle HH, HV \rangle & \langle HH, VV \rangle \\ \langle HV, HH \rangle & \langle HV, HV \rangle & \langle HV, VV \rangle \\ \langle VV, HH \rangle & \langle VV, HV \rangle & \langle VV, VV \rangle \end{bmatrix} \quad (2)$$

where $\langle \bullet \rangle$ represents ensemble average. The polarimetric covariance matrix is a useful feature for distinguishing targets from the background. Since the average of every element is zero,

$$d_c(\underline{X}) = (\underline{X}^*)^T \Sigma_c^{-1} \underline{X} \quad (3)$$

is a weighting distance if the covariance matrix of the background Σ_c is known, where \underline{X}^* is the conjugate of \underline{X} .

When the determinant of the polarimetric covariance matrix of the targets is much larger than that of the background, the distance (3) is a measure of the difference between the targets and the background. In this case, the distance for samples from the background is smaller than the distance for samples from the targets. The distance is also the output of a polarimetric whitening

filter. The properties of the filter are discussed in [3]. In this paper, it is used as a criterion to recognize targets that are of much stronger reflectance than the background.

When $d_c(\underline{X})$ is greater than a threshold T , the sample \underline{X} is considered as a target pixel. The key problem is the choice of the threshold T .

Ulaby [4] statistically models the background, which is usually called clutter in the radar literature. The distance $d_c(\underline{X})$ is also statistically modeled. Since the background is not uniform and the backscattering amplitude from the background fluctuates, a CFAR detector is adopted.

For a given pixel, called the pixel under test (PUT), its neighboring pixels, called the reference pixels, are used to calculate test statistics [5] or to estimate the parameters in the probability density function (PDF) [6]. The threshold for a fixed false alarm rate is obtained from the statistical model. If the distance for PUT is greater than the threshold, PUT belongs to the target.

The spatial relations between PUT and the reference pixels is shown in Figure 1, where $d(u, v)$ is PUT and is located at the center. The window is called the reference window and its size is

$d(u - p, v - q)$	\cdots	$d(u - p, v)$	\cdots	$d(u - p, v + q)$
$d(u - p + 1, v - q)$	\cdots	$d(u - p + 1, v)$	\cdots	$d(u - p + 1, v + q)$
\vdots	\vdots	\vdots	\vdots	\vdots
$d(u, v - q)$	\cdots	$d(u, v)$	\cdots	$d(u, v + q)$
\vdots	\vdots	\vdots	\vdots	\vdots
$d(u + p - 1, v - q)$	\cdots	$d(u + p - 1, v)$	\cdots	$d(u + p - 1, v + q)$
$d(u + p, v - q)$	\cdots	$d(u + p, v)$	\cdots	$d(u + p, v + q)$

Figure 1: Spatial Position of Reference Pixels and the Pixel Under Test.

$Q_w \times P_w$. All of the pixels in the reference window except $d(u, v)$ are reference pixels. The number of reference pixels is $Q_w \times P_w - 1$, where $P_w = (2 \times p + 1)$ and $Q_w = (2 \times q + 1)$.

The CFAR detector has been widely used in radar applications [5, 6, 7, 8]. It adapts the threshold automatically to the local background in an attempt to maintain an approximately constant false alarm rate. Traditional CFAR algorithms are used for point targets and are applied to multi-look SAR images in order to reduce the effects of speckle noise [5, 6, 7, 8]. They are not suited for single-look, high-resolution SAR images. For the purpose of recognition, we emphasize the single-look case because multi-look SAR images are usually obtained by reducing spatial resolution and a portion of the information is lost. We also emphasize high-resolution because targets have some extension in high-resolution SAR images and much more information on the targets is available

than in low-resolution images.

When CFAR detectors are applied to single-look, high-resolution SAR images, several shortcomings remain. Firstly, extended targets disappear because backscatterers from the targets are used to calculate the required statistics. Secondly, it takes a long time to complete detection because of pixelwise computation of the statistics. Thirdly, false targets can be found almost everywhere due to the presence of speckle in SAR images. Finally, the full backscattering patterns from targets are missed because some backscatterers from targets are not much stronger than the local clutter. To solve these problems, a two stage CFAR detector is designed here.

The performance of a CFAR detector depends on the correctness of the statistical model because the calculation of the threshold is based on the assumptions that the PDF of the background is known except for some parameters and that the reference pixels are independent of each other. The performance may be degraded if an incorrect statistical model is used. It is preferable to perform a goodness-of-fit test and an independence test.

The organization of this paper is as follows. Section 2 describes the goodness-of-fit test and the independence test. The two stage CFAR detector and conditional dilation algorithms are described in Section 3. Experimental results are reported in Section 4. Conclusions and future research directions are briefly described in Section 5.

2 STATISTICAL TESTS

The Rayleigh [4], the log-normal [4], the Weibull [4, 5, 6, 7], and the K distribution [8] are all used in radar applications to describe the amplitude or intensity of backscatterers statistically. The Weibull distribution can be made to approach either the Rayleigh or the log-normal distribution [7]. The Rayleigh distribution is also a special case of the K distribution. Recent papers focus on the K distribution and the Weibull distribution. The K distribution is usually used for sea background [8]. Our goal is to detect stationary man-made objects on land, so we use the Weibull distribution. In this paper, the CFAR detector is based on the distance $d_c(\underline{X})$. In order to show the validity of the Weibull distribution for the distance, a Kolmogorov-Smirnov (K-S) test [9] is used as a goodness-of-fit test.

Assume that y_0, \dots, y_{n-1} are n independent samples from the same distribution and that the cumulative distribution function is $F(Y)$. Let $F_n(Y)$ be the sampled cumulative distribution func-

tion. The samples are ordered as $y_{(0)} \leq y_{(1)} \leq \dots \leq y_{(n-1)}$ and then

$$F(y_i) = \text{Prob}\{y \leq y_{(i)}\} \quad (4)$$

$$F_n(y_i) = i/n \quad (5)$$

and

$$M_n = \max_{y_i} |F_n(y_i) - F(y_i)| \quad (6)$$

are computed for the test. When the samples actually belong to the distribution being tested for, the probability of

$$P = \text{Prob}(M_n \geq c) \quad (7)$$

is shown in Table 1^a.

Table 1: Significant Levels

P	0.01	0.05	0.10	0.15	0.20
c	1.63	1.36	1.22	1.14	1.07

For the Weibull case, the probability density function is

$$f(y) = \frac{C}{B} \left(\frac{y}{B}\right)^{C-1} \exp \left[- \left(\frac{y}{B}\right)^C \right] \quad (8)$$

and the cumulative distribution function is

$$F(Y) = 1 - \exp \left(- \left(\frac{Y}{B}\right)^C \right) \quad (9)$$

where C is the shape parameter and B is the scale parameter. When $C = 2$, it is a Rayleigh distribution, and when $C = 1$, it is an exponential distribution. Given the parameters C and B and the independent samples, a confidence test on the Weibull distribution can be set up according to Table 1 and (8) and (9).

When CFAR is implemented, it is required that the samples be independent. The sample correlation coefficient [9] is used. The smaller the sample correlation coefficient is, the less correlated the data are. Although decorrelation is a necessary but not a sufficient condition for independence, it is commonly used due to the simplicity of computing correlation coefficients. Since the data

^aThis table is from [10].

in this paper are from non-Gaussian distributions, it is difficult to set a confidence level for the decorrelation test. Therefore, decorrelation of the data is performed only when the data fail to pass the goodness-of-fit test regardless of the values of the correlation coefficients. Decorrelation for every stage of the CFAR detector is considered in Section 3.

3 THE CFAR DETECTOR

In a CFAR detector, the absolute amplitude makes no sense. The square root of the distance is scaled to make the root representable by integers without loss of significant bits. In the rest of this paper, the scaled square root of the distance is used and is represented as an integer $d(u, v)$, where u and v denote a given spatial position in the image, $u = 0, \dots, U - 1$ and $v = 0, \dots, V - 1$.

As described in Section 2, the Weibull distribution is used to model $d(u, v)$. In practice, C and B in (8) are unknown and they vary with spatial position (u, v) . To make the threshold adapt to the variations, a CFAR detector is used. An order statistic (OS) CFAR algorithm [5] is proposed for the Weibull distribution. This algorithm exhibits extensive CFAR loss [6]. Ravid and Levanon [6] suggest a maximum-likelihood CFAR detector for a Weibull background. In this algorithm [6], the threshold is calculated according to the maximum-likelihood estimation of C and B . This algorithm is adopted to calculate the threshold in this paper, but the method of getting the reference pixels is different.

Suppose that there are n samples in the reference window of PUT, say d_0, \dots, d_{n-1} . The samples come either from the background or from targets. If the samples from targets are used to estimate the statistical parameters, the performance of CFAR will be degraded. To reduce this degradation, the $l\%$ smallest samples are used to estimate the parameters, and the $(100 - l)\%$ largest samples, which might come from targets, are not used. The samples are ordered as $d_{(0)} \leq d_{(1)} \dots \leq d_{(n-1)}$, and $L = l\% \times n$ is calculated. The maximum-likelihood estimate [6] of C satisfies

$$\frac{\sum_{j=0}^{L-1} d_{(j)}^{\hat{C}} \ln d_{(j)}}{\sum_{j=0}^{L-1} d_{(j)}^{\hat{C}}} - \frac{1}{\hat{C}} = \frac{1}{L} \sum_{j=0}^{L-1} \ln d_{(j)} \quad (10)$$

Solving this equation iteratively, as shown in the Appendix, we obtain the estimated parameter \hat{C} and then the estimated parameter \hat{B} from

$$\hat{B} = \left(\frac{1}{L} \sum_{j=0}^{L-1} d_{(j)}^{\hat{C}} \right)^{\frac{1}{\hat{C}}} \quad (11)$$

From \hat{C} and \hat{B} , the threshold

$$T = \begin{cases} (\ln P_{FA})^{\frac{1}{c}} \hat{B} & \text{if } L \geq 120 \\ (\frac{120}{L} \ln P_{FA})^{\frac{1}{c}} \hat{B} & \text{if } L < 120 \end{cases} \quad (12)$$

is obtained, where P_{FA} is the predefined false alarm rate.

In this paper, the algorithm for parameter estimation is slightly different from the algorithm proposed by Ravid and Levanon [6] in that we discard the $(100 - l)\%$ largest samples whereas Ravid and Levanon [6] set them equal to the largest of the $l\%$ smallest samples. It is unlikely that one value occurs many times in a small window since the dynamic range of the SAR image is large. Therefore, it is more reasonable to discard the largest samples than to set them equal to the same value since the largest samples might come from targets and the statistical parameters should be estimated using data from the background.

In our algorithm, the samples are also ordered. But it is different from the algorithm in [5] in the method used to get the threshold. The $l\%$ smallest order statistics are used in this paper, while only two are used in [5]. The performance analysis of the maximum-likelihood algorithm can be found in [6].

As mentioned in Section 1, traditional CFAR algorithms have shortcomings when they are applied to single-look, high-resolution SAR images. To improve detection, CFAR detection is performed twice. The CFAR detection algorithms are described in the following subsections.

3.1 THE GLOBAL CFAR DETECTOR

The $k\%$ smallest pixels in the whole image are used to estimate C and B in (8). We refer to this CFAR as global. The predefined parameters are k and the false alarm rate P_{FA}^{GC} . The threshold is the same for the whole image, and CFAR is not a proper name for the detector since the threshold does not change with spatial position. However, the method used to get the threshold is the same as in CFAR, so we still adopt the name CFAR.

When the global CFAR detector is used, spatial correlation must be considered before doing the goodness-of-fit test and obtaining the threshold. A straightforward way to decorrelate the data is to divide the image into small windows, to compute the correlation coefficients between any two of these windows [9], and to select windows whose correlation coefficients with each other are small. However, this method is impractical. For a 1024×256 image, $1023!$ correlation coefficients would need to be computed if the size of the small windows is 16×16 . To prevent this burdensome

computation, a very simple method is used in this paper. Since the dynamic range of SAR images is large and a single value seldom occurs many times in one small spatial window, samples with the same value are considered to be a single sample and samples with different values are used to do the goodness-of-fit test and to estimate the statistical parameters. The global CFAR algorithm is then the following.

- Algorithm I.

1. Find the maximum value D_{\max} and the minimum value D_{\min} of the image $d(u, v)$ and then compute the histogram $h(d)$ of the image, where $h(d)$ is the number of times that value d occurs in the image and $d = D_{\min}, \dots, D_{\max}$.
2. Find the minimum D which makes $\sum_{d=D_{\min}}^D h(d) \geq k\% \times V \times U$. The image size is $V \times U$.
3. Let $h'(d) = 1$ if $h(d) > 1$, where $d = D_{\min}, \dots, D$.
4. Calculate $L = \sum_{d=D_{\min}}^D h'(d)$.
5. Order the samples as $d_{(0)} < d_{(1)} < \dots < d_{(L-1)}$, where $h'(d_{(i)}) = 1$ and $D_{\min} \leq d_{(i)} \leq D$ for $i = 0, \dots, L - 1$.
6. Substitute samples $d_{(i)} (i = 0, \dots, L - 1)$ into (10) and use the iterative function in the Appendix to get \hat{C} . \hat{B} is obtained by substituting the samples and \hat{C} into (11).
7. Substitute the predefined false alarm rate P_{FA}^{GC} and the estimated parameters \hat{C} and \hat{B} into (12) and obtain the threshold T .
8. Set $GC(u, v) = 0$ if $d(u, v) \leq T$. Otherwise set $GC(u, v) = 1$, where $u = 0, \dots, U - 1$ and $v = 0, \dots, V - 1$.

If $GC(u, v) = 1$, the pixel $d(u, v)$ is accepted as a target pixel in the global CFAR detector. Otherwise, it belongs to the background.

When the goodness-of-fit test is needed, the estimated parameters \hat{C} and \hat{B} and the samples $d_{(i)} (i = 0, \dots, L - 1)$ are used to compute M_n in (6). The value of M_n is reported in Section 4.

3.2 THE LOCAL CFAR DETECTOR

The pixels which are accepted as targets by the global CFAR detector will be detected again using another CFAR detector. In order to distinguish the CFAR detector in this subsection from that in

the previous subsection, the name “local CFAR” is used in this subsection because the threshold is calculated according to local statistical parameters.

When the local CFAR detector is used, the value of M_n is much smaller than that in the global CFAR detector and correlation need not be considered since data in small windows are used to estimate the statistical parameters. If the data in some windows cannot pass the goodness-of-fit test, an auto-regression model is used to decorrelate the data.

If $GC(u, v) = 1$, that is, pixel $d(u, v)$ is accepted as a target by the global CFAR detector, the $l\%$ smallest samples in the reference window are used to estimate C and B in (8). The threshold T is calculated according to the predefined false alarm rate P_{FA}^{LC} . If $d(u, v) > T$, the pixel $d(u, v)$ is accepted as a target pixel. Otherwise, it is rejected as a target pixel. The value of T varies with spatial position (u, v) .

When extended targets are present, there are reference windows in which most of the pixels are already thought to be targets by the global CFAR detector. If the pixels which have been accepted as targets by the global CFAR detector were to be used, the detection would be unreliable since these pixels might come from targets and should not be used to estimate the statistical parameters. In this case, we enlarge the reference window until the number of pixels which are rejected as targets by the global CFAR detector is large enough.

Two algorithms are used in the implementation of the local CFAR detector. In one, the size of the reference window is fixed, and in the other the size of the reference window varies with the position of PUT. The former is used for point targets and the latter is used for extended targets. It is easier to implement the former than to implement the latter. However, the former cannot be used for extended targets. We prefer the latter algorithm since it can be used for both point targets and extended targets. The drawback of the latter algorithm is that false targets might occur in the detected image.

The two algorithms are implemented in the following steps.

- Algorithm II (Point targets).

1. Calculate $n = Q_w \times P_w - 1$ and $L = l\% \times n$.
2. For every pair (u, v) , do the following steps if $GC(u, v) = 1$. Otherwise set $LC(u, v) = 0$, where $u = 0, \dots, U - 1$ and $v = 0, \dots, V - 1$.
3. Order the reference pixels as $d_{(0)} \leq d_{(1)} \dots \leq d_{(n-1)}$.

4. Substitute samples $d_{(i)}(i = 0, \dots, L - 1)$ into (10) and use the iterative function in the Appendix to get \hat{C} . \hat{B} is obtained by substituting the samples and \hat{C} into (11).
5. Substitute the predefined false alarm rate P_{FA}^{LC} and the estimated parameters \hat{C} and \hat{B} into (12) and compute the threshold T . This threshold changes with spatial position (u, v) , but the false alarm rate does not change.
6. Set $LC(u, v) = 0$ if $d(u, v) \leq T$. Otherwise set $LC(u, v) = 1$.

If the distribution test needs to be performed, calculate M_n in (6) instead of the threshold T in Step 5 .

- Algorithm III. (Extended targets)

1. Calculate $L = l\% \times Q_w \times P_w - 1$. The smallest size of the reference window is $Q_w \times P_w$.
2. For every pair (u, v) , do the following steps if $GC(u, v) = 1$. Otherwise set $LC(u, v) = 0$, where $u = 0, \dots, U - 1, v = 0, \dots, V - 1$.
3. Set $P = P_w$ and $Q = Q_w$. The size of the reference window is $Q \times P$.
4. Order the reference pixels as $d_{(0)} \leq d_{(1)} \dots \leq d_{(n-1)}$, where $n = Q \times P - 1$.
5. Do the following if there exists at least one pixel (i, j) in the reference window which satisfies $GC(i, j) = 0$ and $d(i, j) = d_{(L-1)}$. Otherwise set $P = P + 2$ and $Q = Q + 2$ and go back to Step 4 to find new reference pixels in the enlarged reference window.
6. Substitute samples $d_{(i)}(i = 0, \dots, L - 1)$ into (10) and use the iterative function in the Appendix to get \hat{C} . \hat{B} is obtained by substituting the samples and \hat{C} into (11).
7. Substitute the predefined false alarm rate P_{FA}^{LC} and the estimated parameters \hat{C} and \hat{B} into (12) and compute the threshold T . This threshold changes with spatial position (u, v) , but the false alarm rate does not change.
8. Set $LC(u, v) = 0$ if $d(u, v) \leq T$. Otherwise set $LC(u, v) = 1$.

If the distribution test needs to be performed, calculate M_n in (6) instead of the threshold T in Step 7 .

As in the global CFAR detector, a pixel $d(u, v)$ is accepted as a target pixel if $LC(u, v) = 1$. Otherwise, it is rejected as a target pixel.

3.3 CONDITIONAL DILATION

Conditional dilation is performed according to the binary images $GC(u, v)$ formed in the global CFAR detector and $LC(u, v)$ formed in the local CFAR detector.

If a pixel is accepted as a target pixel by the local CFAR detector, all the pixels connected to it will also be accepted as target pixels if these pixels are accepted as target pixels by the global CFAR detector. Doing this is based on the following considerations.

Since the impulse response of a target to the incident wave is not a $\delta(t)$ function and neither is the incident wave, the backscatterers from the target are distributed in a region instead of at one pixel. But the backscattering is very strong only at a few pixels. To see the pattern of backscattering from the target clearly, we prefer to retrieve the pixels which are backscatterers from the target but are not much stronger than the backscatterers from the neighboring background. These pixels should be extracted by the global CFAR detector since the $k\%$ smallest pixels in the whole image, not only the neighbors of the target, are used to get the threshold.

The algorithm for conditional dilation based on 8-neighbors is described as follows.

- Algorithm IV.

1. Scan the first row from left to right to find all the continuous intervals in which (and at the endpoints of which) the values of $GC(u, v)$ are all equal to one but the values of $LC(u, v)$ are all equal to zero. Let $[v_1, v_2]$ be such an interval. This description can be expressed as $GC(0, v) = 1$ and $LC(0, v) = 0$ for any $v \in [v_1, v_2]$. Note that a special case is $v_1 = v_2$.
2. Set $LC(0, v) = 1$ for any $v \in [v_1, v_2]$ if $LC(0, v_1 - 1) = 1$ or $LC(0, v_2 + 1) = 1$, where $[v_1, v_2]$ is an interval found at the first step. This is repeated for all the intervals found at the first step.
3. Do the following, beginning at $u = 1$ and ending at $u = U - 1$. Find all the intervals in the u -th row as in the first step. Set $LC(u, v) = 1$ for any $v \in [v_1, v_2]$ if $LC(u, v_1 - 1) = 1$ or $LC(u, v_2 + 1) = 1$ or there exists an m such that $LC(u - 1, m) = 1$, where $m \in [v_1 - 1, v_2 + 1]$ and $[v_1, v_2]$ is an interval found in the u -th row. This is repeated for all the intervals found in the u -th row.
4. Do the following, beginning at $u = U - 2$ and ending at $u = 0$. Find all the intervals in the u -th row as in the first step. Set $LC(u, v) = 1$ for any $v \in [v_1, v_2]$ if $LC(u, v_1 - 1) = 1$

or $LC(u, v_2 + 1) = 1$ or there exists an m such that $LC(u + 1, m) = 1$, where $m \in [v_1 - 1, v_2 + 1]$ and $[v_1, v_2]$ is an interval found in the u -th row. This is repeated for all the intervals found in the u -th row.

5. The third and fourth steps are repeated until no pixel whose value is equal to one in $GC(u, v)$ and is equal to zero in $LC(u, v)$ is set to one after dilation at both the third and fourth steps.

The binary image $LC(u, v)$ which is obtained after dilation is the final result.

4 EXPERIMENTAL RESULTS

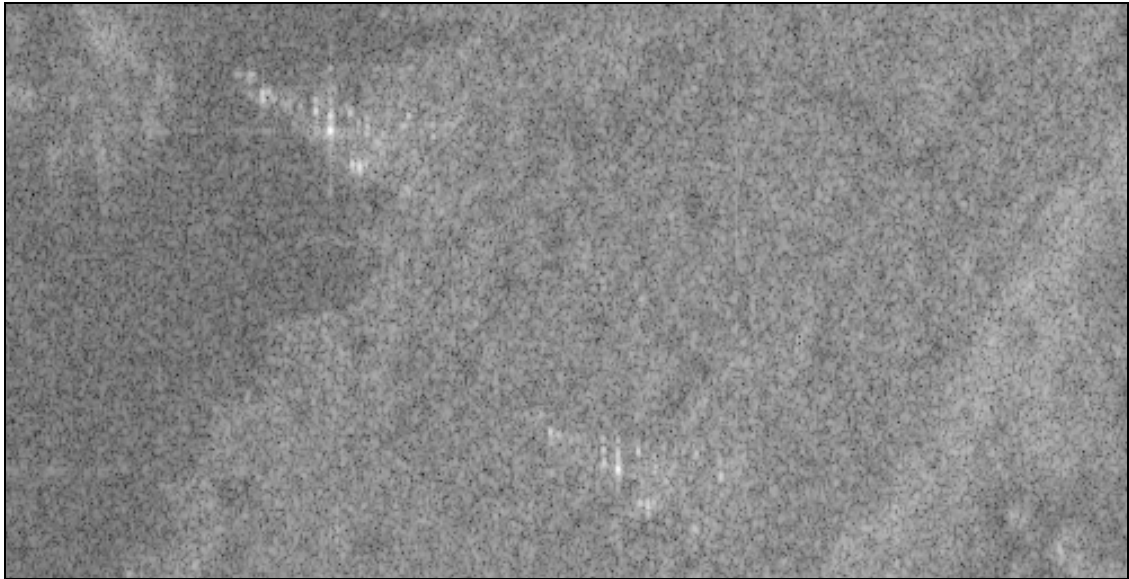
Three single-look, fully polarimetric SAR images obtained from Dr. Les Novak of MIT Lincoln Laboratory were used. The resolution is 1ft by 1ft and the size is 1024×256 . Due to space limitations, only a portion of each image is displayed. The original SAR images are shown in (a) of Figures 2, 3 and 4. The man-made objects with strong backscattering in these images are powerlines, bridge fences, metallic guard rails, and buildings.

We have estimated the polarimetric covariance matrix of the background using raw data.

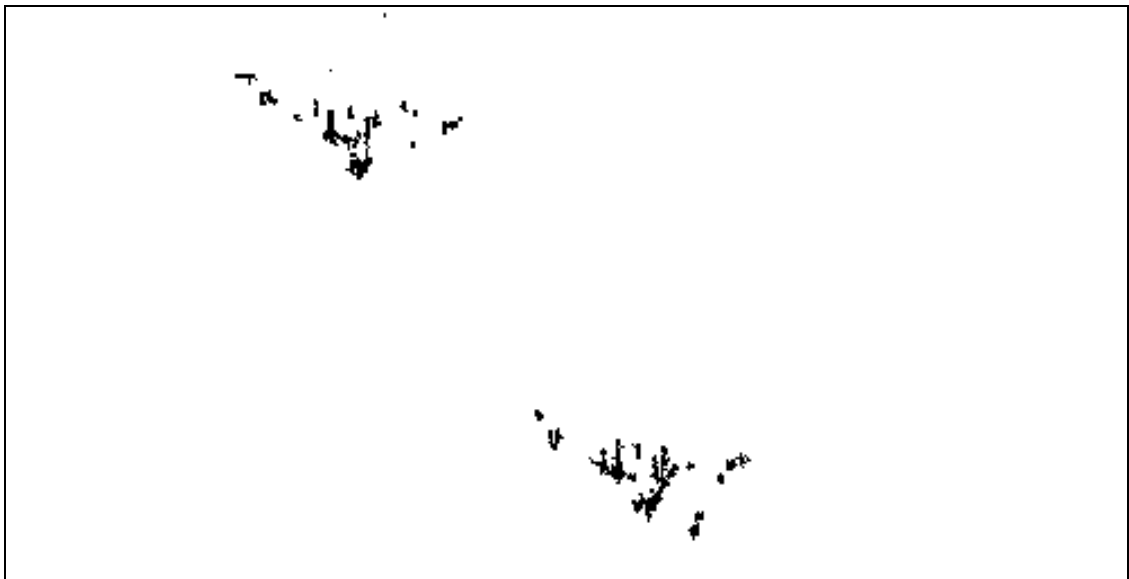
$$\Sigma_c = \begin{bmatrix} 1 & 0 & 0.8 \\ 0 & 0.2 & 0 \\ 0.8 & 0 & 1 \end{bmatrix} \quad (13)$$

is a good approximation to the polarimetric covariance matrix for different types of background. In (13), the matrix has been normalized to make the first element equal to 1.

For all three images, $k = 60$, $P_{FA}^{GC} = 10^{-6}$, $P_{FA}^{LC} = 10^{-7}$, $l = 90$, $P_w = 11$ and $Q_w = 11$. No other parameters are required for the CFAR detectors. In the local CFAR detector, the algorithm for point targets is used for the images in Figures 2 and 3 and the algorithm for extended targets is used for the image in Figure 4. The final detection results are shown in (b) of Figures 2, 3 and 4. For illustration purposes, the black dots are used to denote targets with strong backscattering in the detected images. The results of the distribution test are shown in Table 2. In the global CFAR detector, the value of M_n in (6) before decorrelation is given in the second row and the value after decorrelation is given in the third row. The maximum value of M_n for all the pixels under test in the local CFAR detector is shown in the fourth row. The number of pixels under test in the local CFAR detector is given in the fifth row. The number of pixels under test whose reference pixels fail



(a) SAR Image

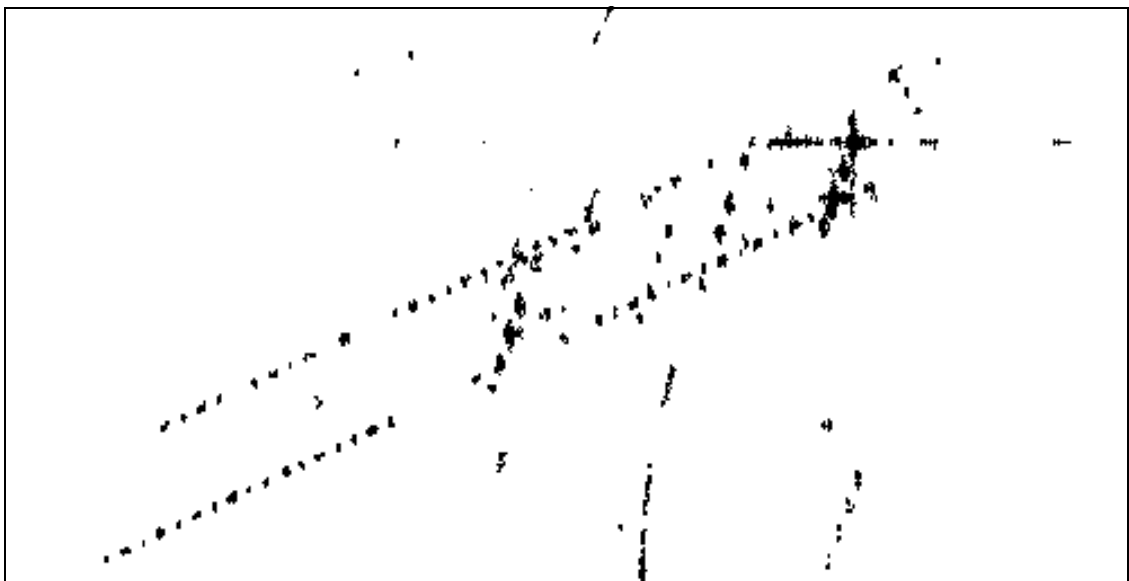


(b) Detected Image

Figure 2: Powerlines

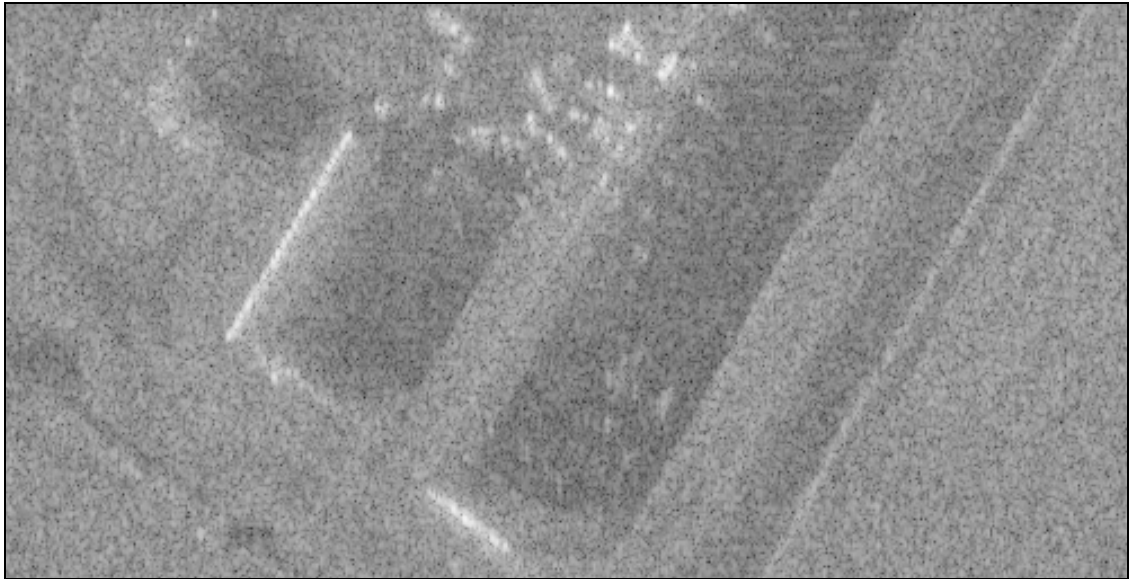


(a) SAR Image

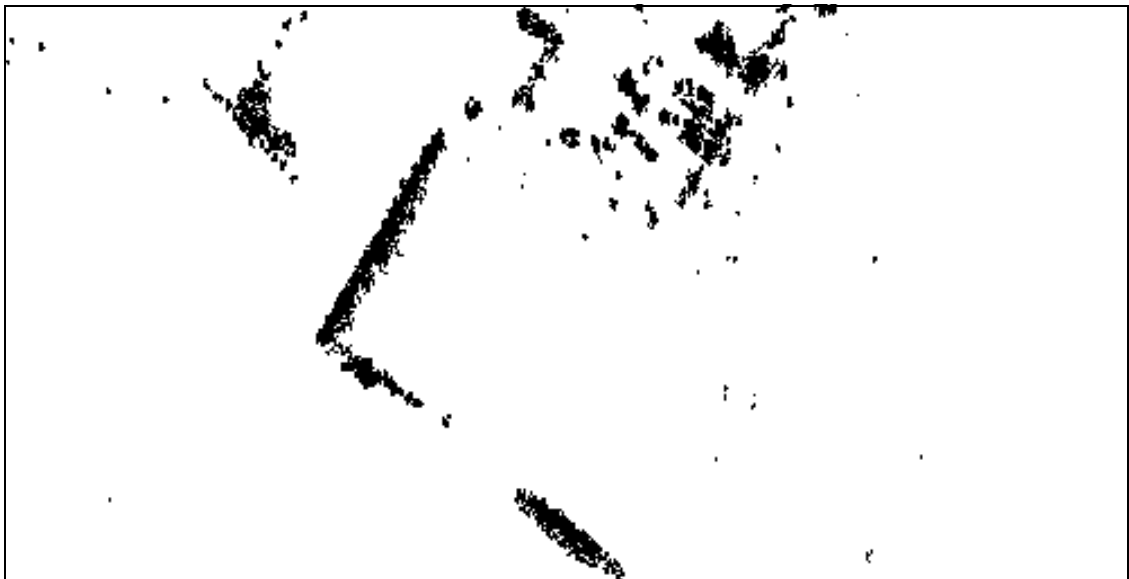


(b) Detected Image

Figure 3: Bridge Fences and Metallic Guard Rails



(a) SAR Image



(b) Detected Image

Figure 4: Buildings

Table 2: Results of Distribution Test

Figure	2	3	4
M_n B. D.	18.09	16.47	23.56
M_n A. D.	2.78	3.23	2.97
M. M_n	2.03	2.18	1.70
N. PUT	18705	13398	8855
N. F. P_1	18	110	1
N. F. P_2	908	1326	188

to pass the distribution test is shown in the last two rows. The next to the last row is for $P = 0.05$; see (7). The last row is for $P = 0.20$.

If the pixels whose reference pixels fail to pass the distribution test are displayed, we can see that most of the pixels are target pixels and the rest are neighbors of target pixels when $P=0.05$.

5 SUMMARY

Compared with other detection algorithms, the method proposed in this paper has the following advantages. Single-look data are used instead of multi-look data so that the resolution of the SAR images remains; the pattern of backscattering from the targets is kept, and small targets, which may disappear in multi-look data, are kept in the detected images. The effects of speckle are removed by the global CFAR detector. The full pattern of backscattering from the targets is retrieved by conditional dilation. Extended targets are extracted since the size of the reference window varies with spatial position. Compared with other algorithms, fewer computations are required. In the global CFAR detector, the ordering is realized by computing the histogram, and the computation is fast. As shown in Table 2, the numbers of pixels required to do the detection in the local CFAR detector are 18705, 13398 and 8855 for Figures 2, 3 and 4 respectively. Therefore, the computation in the local CFAR detector is much faster than in other algorithms, where the local statistical parameters for each of the 1024×256 pixels in the image need to be calculated.

The polarimetric covariance matrices in different regions of the background are used to do the detection. The detection results are almost the same using our method, whereas false targets occur almost everywhere with other algorithms due to improper polarimetric covariance matrices. Thus, our method is robust compared with other algorithms.

From Table 2, we see that the decorrelation is successful in the global CFAR detector. The

assumption that the background is Weibull distributed is reasonably good according to the experimental results.

In practice, the polarimetric covariance matrix of the background is not known beforehand and the matrix changes from one region to another in the SAR images. It is desirable to design an algorithm in which both the threshold for detection and the polarimetric covariance matrix adapt to variations in the background.

For the CFAR algorithm, detection performance also depends on the false alarm rate. If the rate is too large, targets may be lost. If it is too small, false targets may be found almost everywhere. To solve this, one idea is to compute sample polarimetric covariance matrices for every region which is recognized as a target by the CFAR algorithm and compare them with a priori information on the background and the target. However, the matrices of some targets are very similar to that of the background. This makes it difficult to distinguish targets from the background using the polarimetric covariance matrix.

References

- [1] R. D. Chaney, M. C. Burl and L. M. Novak, On the performance of polarimetric target detection algorithms, IEEE International Radar Conference, Arlington, VA, 1990, 520–525.
- [2] F. T. Ulaby and C. Elachi, *Radar Polarimetry for Geoscience Applications*. Norwood, MA: Artech House, 1990.
- [3] L. M. Novak and M. C. Burl, Optimal speckle reduction in POL-SAR imagery, IEEE Trans. on Aerospace and Electronic Systems, Vol. 25, No. 2, March, 1989, 150–165.
- [4] F. T. Ulaby and M. C. Dobson, *Handbook of Radar Scattering Statistics for Terrain*. Norwood, MA: Artech House, 1989.
- [5] N. Levanon and M. Shor, Order statistics CFAR for Weibull background, IEE Proceedings-F, Vol. 137, No. 3, June, 1990, 157–162.
- [6] R. Ravid and N. Levanon, Maximum-likelihood CFAR for Weibull background, IEE Proceedings-F, Vol. 139, No. 3, June, 1992, 256–264.
- [7] D. C. Schleher, Radar detection in Weibull clutter, IEEE Trans. on Aerospace and Electronic Systems, Vol. 12, No. 6, November, 1976, 736–743.

- [8] B. C. Armstrong and H. D. Griffiths, CFAR detection of fluctuating targets in spatially correlated K-distributed clutter, IEE Proceedings-F, Vol. 138, No. 2, April, 1991, 139–152.
- [9] A. Stuart and J. K. Ord, *Advanced Theory of Statistics*, Vol. 2, New York: Oxford University Press, 1991.
- [10] G. W. Lank and N. M. Chung, CFAR for homogeneous part of high-resolution imagery, IEEE Trans. on Aerospace and Electronic Systems, Vol. 28, No. 2, April, 1992, 370–381.
- [11] J. F. Traub, *Iterative Methods for the Solution of Equations*. Englewood Cliffs, NJ, Prentice-Hall, 1964.

Appendix

It is straightforward to use the one-point iterative function [11]

$$\frac{1}{C_{m+1}} = \frac{\sum_{j=0}^{L-1} d_{(j)}^{C_m} \ln d_{(j)}}{\sum_{j=0}^{L-1} d_{(j)}^{C_m}} - \frac{1}{L} \sum_{j=0}^{L-1} \ln d_{(j)} \quad (14)$$

for estimating C in (10), where the initial value $C_0 = 2$. When the algorithm is implemented, the sequence $\{C_m\}$ is often divergent or its convergence speed is slow. Analyzing these sequences, the following features are discovered:

$$C_m = C + \epsilon_m \quad (15)$$

$$C_{m+1} = C + \epsilon_{m+1} \quad (16)$$

where C is the correct solution of (10). For a divergent sequence, ϵ is an extremely small positive value when m is large enough, and for a sequence whose convergence speed is slow, ϵ is an extremely small negative value when m is large enough. Based on the analysis, a two-point iterative function is adopted:

$$C_{2m+1} = \frac{C_{2m} + C_{2m-1}}{2} \quad (17)$$

where C_{2m} is obtained from the one-point iterative function. The initial values are $C_0 = 1$ and $C_{-1} = 3$. If there exists an M such that

$$\left| \frac{C_{2M-1} - C_{2M}}{C_{2M}} \right| < 0.01 \quad (18)$$

the iteration is terminated and the estimated parameter is

$$\hat{C} = C_{2M} \quad (19)$$

After the two-point iterative function is used, M is less than 10 when the sequence C_m is convergent according to the criterion in (18).